Rivers shaped by the most erosion resistant material

Preprint, compiled June 28, 2019

Kieran B.J. Dunne[1*] **and Douglas J. Jerolmack**[1,2]

[1]Department of Earth & Environmental Science, University of Pennsylvania, Philadelphia, Pennsylvania, USA
[2]Department of Mechanical Engineering & Applied Mechanics, University of Pennsylvania, Philadelphia, Pennsylvania, USA

Abstract

Alluvial rivers are formed by, and are an expression of, the water and sediment that they convey [1, 2]. They are the primary arteries of water and nutrients on land, making them the lifeblood of communities and commerce [3]. While a myriad of environmental and geological factors have been proposed to control alluvial river size [4, 5, 6], near-universal scaling relations between channel geometry and discharge [7] suggest a common organizing principle. Here we use a global dataset, and a novel field study, to support a simple hypothesis [8]: river geometry adjusts to the threshold fluid entrainment stress of the most resistant material lining the channel. This threshold condition describes the averaged hydraulic state of natural rivers, and is compatible with dynamics; erosion and deposition on channel banks, associated with meandering, for example, represent higher-order variations in fluid stress around the mean state [9]. This greatly extends the applicability of threshold channel theory, which was originally developed to explain straight gravel-bedded rivers with uniform grain size and stable banks [1]. We show how increasing the relative threshold of bank to bed material leads to a proportionate reduction in channel width and increase in channel depth; in this manner, muddy banks encourage sand-bedded rivers to adopt a meandering (rather than braided) morphology. The parsimonious "threshold-limiting material" model provides guidance for river management and restoration practices [10], and may aid in the reconstruction of past climates on Earth and other planetary bodies using alluvial river deposits [11].

Main

What controls the width and depth of a river? Despite the need for channel design principles to guide river management and restoration [12, 10], and the rapid development of sophisticated numerical models that simulate landscapes [13], this fundamental question remains unanswered [14]. As a first step toward understanding the shape of natural rivers, Parker [1] proposed a mechanistic solution for the equilibrium geometry of an idealized model system: a straight and trapezoidal channel with constant water discharge, lined with uniform coarse (gravel) material. The resulting channel has stable banks in which the fluid boundary-shear stress at bankfull (Fig. 1C), τ_{bf}, is equal to the threshold for particle entrainment, τ_c. Lateral momentum diffusion accommodates sediment transport in the channel center where $\tau_{bf} \approx 1.2\tau_c$ (Fig. 1C). The latter provides a closure scheme (Supplementary Materials) that allows one to derive a simplified set of "regime equations" that predict the channel bankfull width, W_{bf}, and depth, H_{bf}, (Fig. 1C), as a function of specified hydraulic variables:

$$W_{bf} = \frac{Q_{bf} S}{C_f g^{1/2} \left(\frac{1.2\tau_c}{\rho g}\right)^{3/2}}, \tag{1}$$

and

$$H_{bf} = \frac{1.2\tau_c}{\rho g S}, \tag{2}$$

where Q_{bf}, S, C_f, g, and ρ are the bankfull discharge, slope, empirical friction factor, acceleration due to gravity, and density of water, respectively (Fig. 1C; see Methods).

The assumptions of the Parker model [1] appear to be incompatible with natural alluvial rivers that are typically sinuous, with heterogeneous bed and bank materials [5, 6] and variable discharge, for which bank erosion and deposition are common (see Supplementary). Nonetheless, the near-threshold closure has been shown to describe hydraulic geometry trends in natural gravel-bedded rivers (here defined as having a median bed-sediment diameter, $D_{50} > 1$ cm) [15, 16]. We suggest that there are two factors that explain this apparent paradox. First is that gravel has a larger entrainment threshold than typical bank materials such as mud [8]; river-bank composition likely influences the rates and style of bank erosion, but not the overall channel size. Second is the idea that the lateral fluid stress profile in a straight channel is representative of the spatially-averaged flow over many cross sections in a curved channel. The uniform flow approximation for boundary stress, $\tau_{bf} = \rho g H_{bf} S$, can only be applied over length

*dengjiamin@gmail.com

*correspondence: dengjiamin@gmail.com

scales significantly larger than individual bends; as pointed out by Dietrich et al. [9], it is the "zero-order stress model". Thus, we consider the Parker model as a mean field theory [17] for the time- and space-averaged geometry of natural gravel-bedded rivers. To illustrate, we consider a reach of the Lochsa River, a gravel-bedded, meandering river in Idaho (Q_{bf} = 446 $m^3 s^{-1}$, D_{50} = 0.15m, S = 0.0023, τ_c = 62.3Pa) [15]. Although there is significant variation in channel width about the mean value ($\langle W_{bf} \rangle$ = 61.4 ± 9.6 m), the latter is within 8% of the value predicted by approximating the river as a straight, trapezoidal channel with uniform grain size, constant discharge and stable banks (Fig. 1C.).

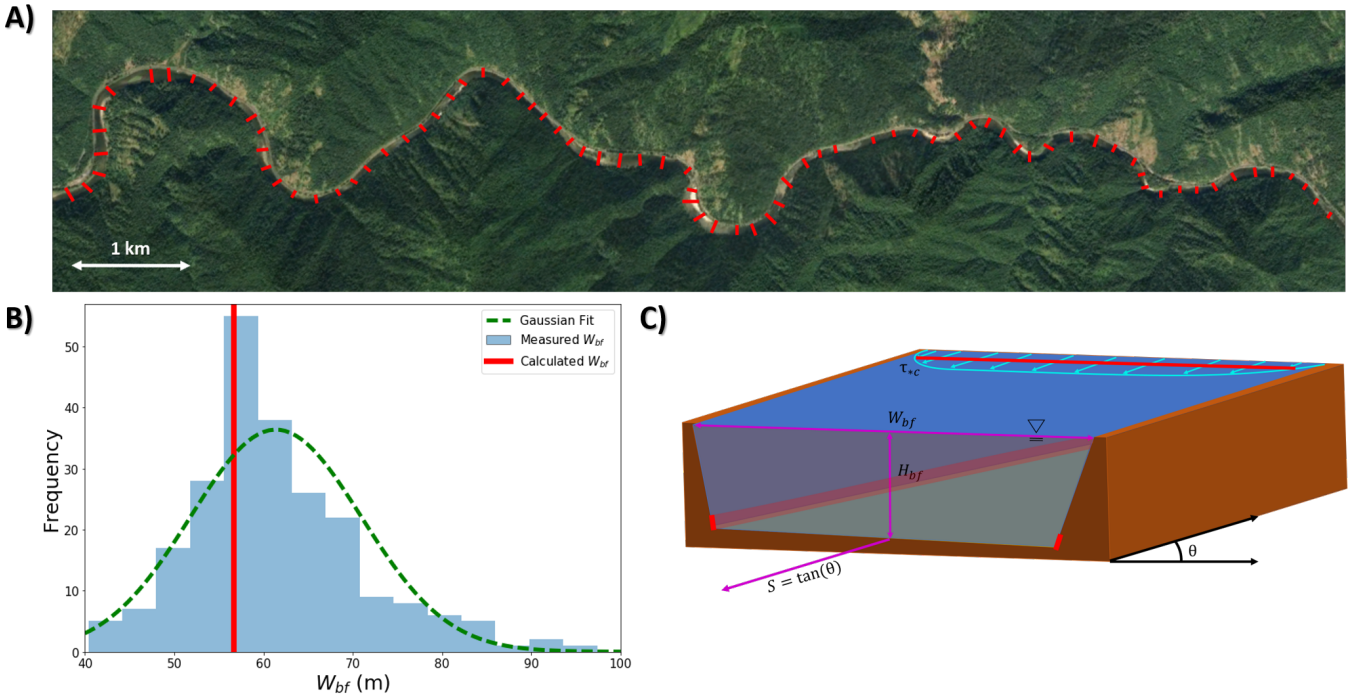

Figure 1: Demonstration of the mean field channel model. A) The Lochsa River, Idaho, USA. Red lines indicate approximately every third measured W_{bf} from Google Earth (Image Source: Google Earth). B) Histogram of W_bf (N = 230). Red line indicates calculated W_{bf} from Eq. 1. C)Schematic of an idealized straight, trapezoidal channel. Cyan lines at surface illustrate lateral boundary fluid-shear stress profile across the channel, τ_{bf}. Red lines at the bank toe show the location where bed and bank materials meet. Horizontal red line intersecting the cyan velocity profile indicates τ_c of the threshold-limiting material. For the Parker model, $\tau_{bf} = \tau_c$ at the bank toe and $\tau_{bf} = 1.2\tau_c$ in the channel center.

For rivers with fine-grained (D_{50} < 1 cm) beds, bankfull fluid stresses typically far exceed the entrainment threshold of bed sediment (i.e, $\tau_{bf}/\tau_c >> 1$) [18, 16]. This condition appears to be incompatible with the Parker model of stable, threshold banks [19, 5]. Recently, however, a generalization of the Parker model has been proposed [8] that we call the "threshold limiting material" model. It states that river geometry adjusts to the threshold entrainment stress of the most resistant material lining the channel. This implies that fine-grained rivers are controlled by τ_c of typically cohesive bank-toe material, which forms the structural anchor of the river bank (Fig. 1C) [8]. We test this model by examining a global data set of river hydraulic geometry [20, 21, 15, 8]. For gravel-bedded rivers having D_{50} > 1 cm, we see that τ_{bf} values cluster around τ_c estimated for river-bed sediments using the Shields curve (Fig. 2A). The significant scatter is likely due to site-specific controls on τ_c that are not accounted for [15]. For rivers with D_{50} < 1 cm, however, we see data peel off of the Shields curve; the smaller the river-bed grain size, the larger τ_{bf} deviates from τ_c [8]. The departure point corresponds to $\tau_{bf} \sim 10^1$ Pa, where we infer that τ_c of cohesive banks becomes larger than τ_c of non-cohesive bed sediments, on average. We also examine the distribution of fluid shear velocity, $U^* = \sqrt{\tau/\rho}$, for flows exceeding bankfull. Phillips and Jerolmack [15] posited that maintenance of a stable average channel geometry requires that U^* values exceeding bankfull (U^*_{bf}) drop off rapidly, and showed for gravel-bedded rivers that this drop off is exponential. While U^* distributions for fine-grained rivers vary widely, normalizing each distribution by U^*_{bf} reveals a trend that is identical to gravel-bedded rivers (Fig. 2), for which $U^*_{bf} \approx 1.1 U^*_c$ (equivalent to $\tau_{bf} \approx 1.2\tau_c$; i.e., the Parker closure). If the threshold limiting material model is correct, this implies that the range of τ_c for bank materials is $3 \leq \tau_c \leq 10$ Pa — in reasonable agreement with reported ranges for muddy river banks in the literature [8, 22]. With this tentative support for the threshold limiting model, we test its ability to predict the width of all of the alluvial rivers in the global dataset, as a function of the imposed parameters slope and discharge. Predictive use of equations 1 and 2 requires assuming values for C_f and τ_c. For gravel-bedded rivers (D_{50} > 1 cm) we apply a constant C_f = 8.69 that is the average value of those channels, while τ_c for each river is determined using the Shields

curve [23]. For fine-grained rivers ($D_{50} < 1$ cm), where we assume that bank cohesion is limiting, we assign a constant $\tau_c = 8$ Pa that is representative of sand-clay mixtures [22], and an average $C_f = 11.12$. Modelled channel widths cluster around measured values (Fig. 2D) for the entire dataset, with fine-grained rivers plotting right on top of gravel-bedded rivers.

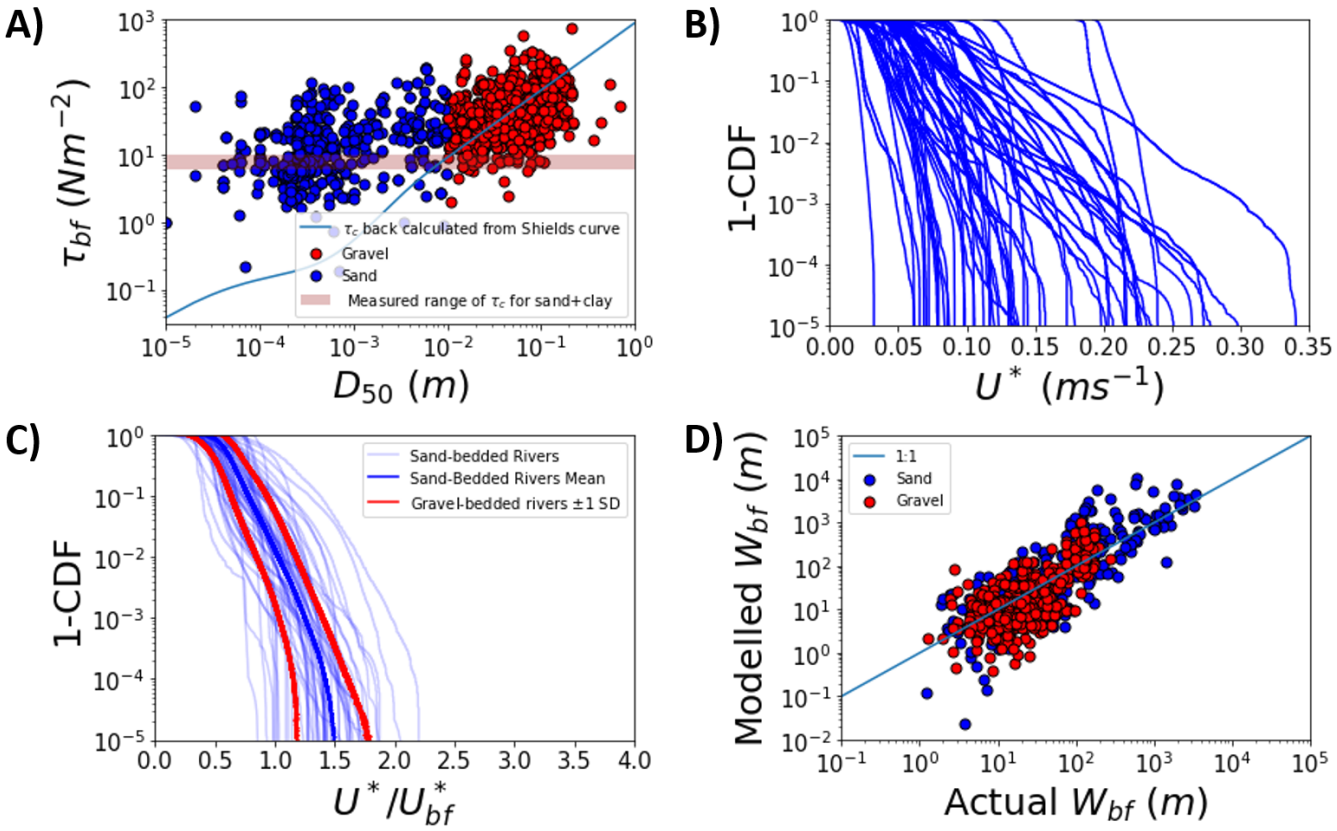

Figure 2: Flow and geometry conditions for the global river data. A) Bankfull shear stress τ_{bf} against median grain size D_{50} for gravel-bedded ($D > 1$ cm) and fine-grained ($D < 1$ cm) rivers. Blue line is τ_c determined from bed D_{50} based on the Shields curve [23]. Pink band shows our experimentally-determined range of τ_c for sand-clay mixtures [22]. Note that gravel-bedded rivers generally follow the Shields curve indicating bed-sediment control, while fine-grained rivers are consistent with cohesive bank control. B) U^* magnitude-frequency distribution for a subset of fine-grained rivers in the global dataset ($n = 56$), showing high variability. C) The same as (B) but normalized by U^*_{bf} for each river. Data collapse along a single curve; the dark blue line is the mean curve of fine-grained rivers, while red lines show standard deviation of gravel-bedded rivers [15] which are nearly identical to the fine-grained dataset. D) Modelled W_{bf} using Eq. 1 vs. measured W_{bf} values for all rivers in the global dataset.

The preceding result provides encouraging, but indirect, evidence that the first-order trend in channel hydraulic geometry may be predicted using the threshold limiting material model. A direct test requires *in-situ* measurement of the fluid entrainment threshold of bank-toe materials in a river with a sand bed and cohesive banks. Up to now, existing methods were either too unwieldy or too indirect to determine τ_c at targeted locations in a channel. We have developed a new instrument, the Mudbuster, that is specifically designed to overcome these shortcomings [22]. Here we report its first field deployment on the Mullica River, a sinuous, single-threaded, sand-bedded river ($D_{50} \approx 0.4$ mm; see Methods, Supplementary Fig. 4) with muddy banks (Fig. 3). We selected a 150-m reach of the river ($Q_{bf} \approx 4.5$ m^{3}s^{-1}, $S = 0.0008$, $W_{bf} \approx 5$ m, $H_{bf} \approx 1.2$ m; see Methods, Supplementary Fig. 5) in which vegetation rooting depths were shallow compared to channel depth, in order to isolate sediment cohesion effects that could be measured directly with the Mudbuster. We surveyed 18 channel cross sections spaced roughly one channel-width apart to determine τ_{bf}, and measured τ_c of the bank-toe material at each station (see Methods). The average value $\tau_c = 4.5$ Pa for bank-toe material (see Supplementary Materials) is over ten times larger than $\tau_c = 0.3$ Pa for non-cohesive sand that makes up the bed [22]. All 18 cross sections are close to $\tau_{bf} = 1.2\tau_c$ (Fig. 3) for the threshold-limiting bank-toe material, but well above threshold for the sand bed. Results from the Mullica River are in striking agreement with the generalized Parker model.

Because of the influence of τ_c on channel width (Eq. 1) and depth (Eq. 2), we anticipate that the threshold-limiting material will exert a first-order control on channel planform morphology. A hydrodynamic stability analysis [2] predicts the transition from single-threaded to multiple-threaded (braided) planform morphologies as a function of Q_{bf}, S, W_{bf}, and H_{bf}. Using our Eq. 1 and

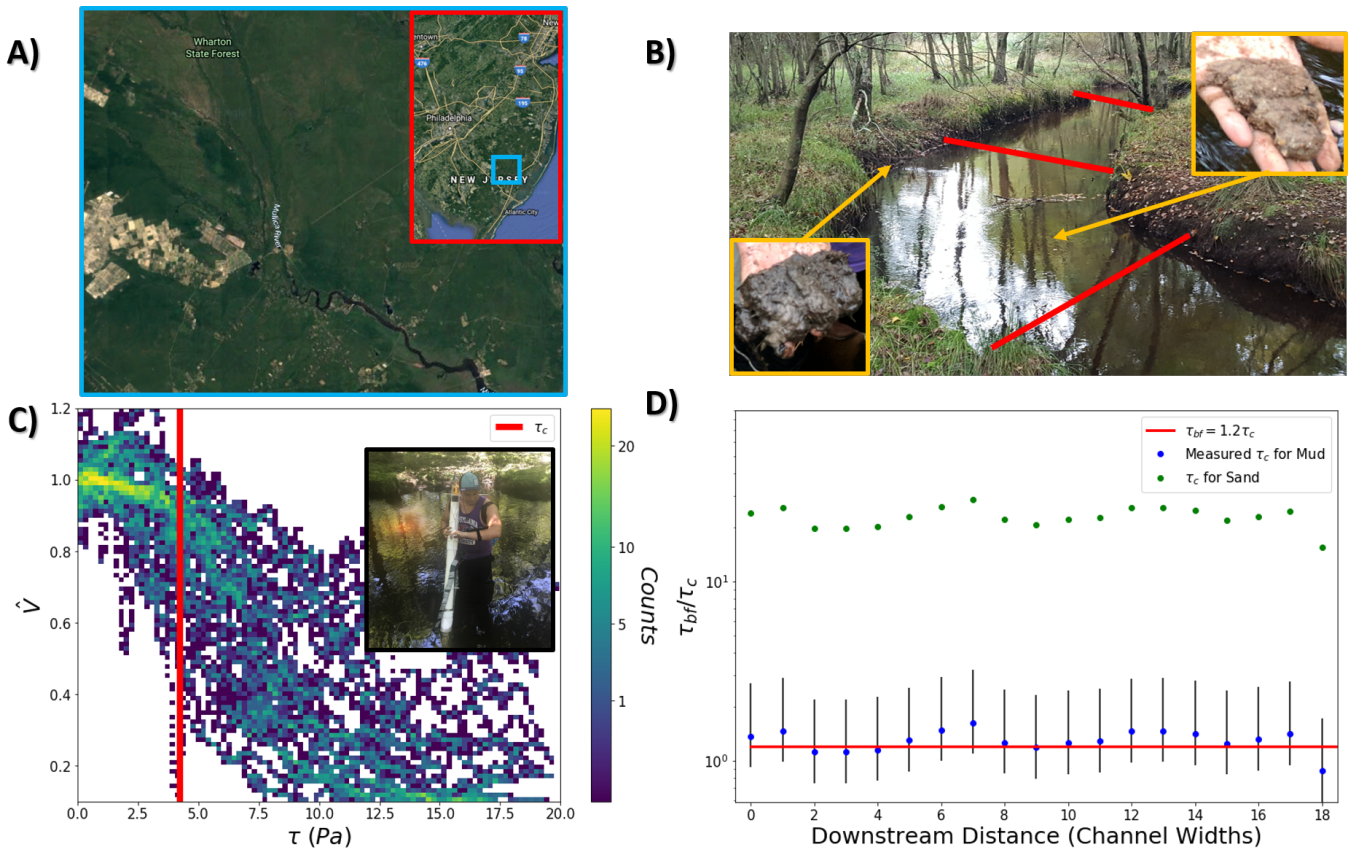

Figure 3: Threshold limiting material case study. A) Location of the Mullica river watershed in Wharton State Forest in the New Jersey coastal plain (Image source: Google Earth). B) Portion of the surveyed reach of the Mullica river. Red lines mark surveyed cross sections. Muddy bank and bed materials shown in bottom left and top right, respectively. C) Mudbuster measurements used to determine τ_c of bank-toe material. The fluid shear stress τ is gradually ramped up, while turbidity is measured as a voltage drop normalized by the initial voltage prior to shearing, $\hat{V}$ [22]. This 2D histogram (colorbar shows counts in each bin) is derived from 28 measurements of bank-toe material; the red line shows the mean value $\tau_c = 4.5$ Pa determined from these data (see Methods). Inset: Implementation of the "Mudbuster" to measure τ_c of bank-toe material; device is controlled using a smart phone via a Bluetooth connection [22]. D) Values of τ_{bf}/τ_c for all 18 cross sections, where $\tau_c = 4.5$ Pa was determined from the average of bank-toe material measurements; the Parker model value $\tau_{bf}/\tau_c = 1.2$ is shown for reference, and error bars indicate ± 1 standard deviation. Green points show $\tau_{bf}/\tau_c >> 1$ for sand-bedded material, indicating control of cohesive bank-toe material on channel geometry.

2, we recast the hydrodynamic stability criterion, ϵ, in terms of the threshold limiting stress τ_c:

$$\epsilon = \frac{Q_{bf} S^{5/2} g^2 \rho^{5/2}}{\pi C_f^2 (1.2\tau_c)^{5/2}}, \tag{3}$$

where we expect braiding for $\epsilon > 1$, and a single-thread morphology for $\epsilon < 1$ [2]. Our global dataset is composed almost exclusively of US Geological Survey gaging stations placed in single-threaded channels, and should therefore plot overwhelmingly below the $\epsilon = 1$ plane in the phase space of the imposed variables Q_{bf}, S and τ_c (Fig. 4C). We compute ϵ for all rivers, using the Shields curve to determine τ_c and a fixed global average value $C_f = 9.74$. Almost all of the gravel rivers (392/406) plot below the $\epsilon = 1$ plane; i.e., the expected morphology agrees with observations. In contrast, most of the fine-grained rivers (264/305) plot above the $\epsilon = 1$ plane; i.e., the predicted braided morphology is not what is observed. Assuming a representative cohesive bank entrainment threshold of $\tau_c = 8$ Pa, however, shifts almost all of the fine-grained rivers (279/305) into the single-threaded regime. The assumption of a fixed τ_c for bank materials is, of course, a crude assumption. We find that improved knowledge of site-specific τ_c results in better predictions (Fig. 4B). These results provide an explanation for the observation that single-threaded, sand-bedded rivers in nature and the laboratory [24] seem to require cohesive and/or vegetated banks.

Our findings indicate that average alluvial river geometry may be predicted with knowledge of four parameters: bankfull discharge, slope, friction factor, and entrainment stress of the the threshold limiting material. More refined models for determining C_f

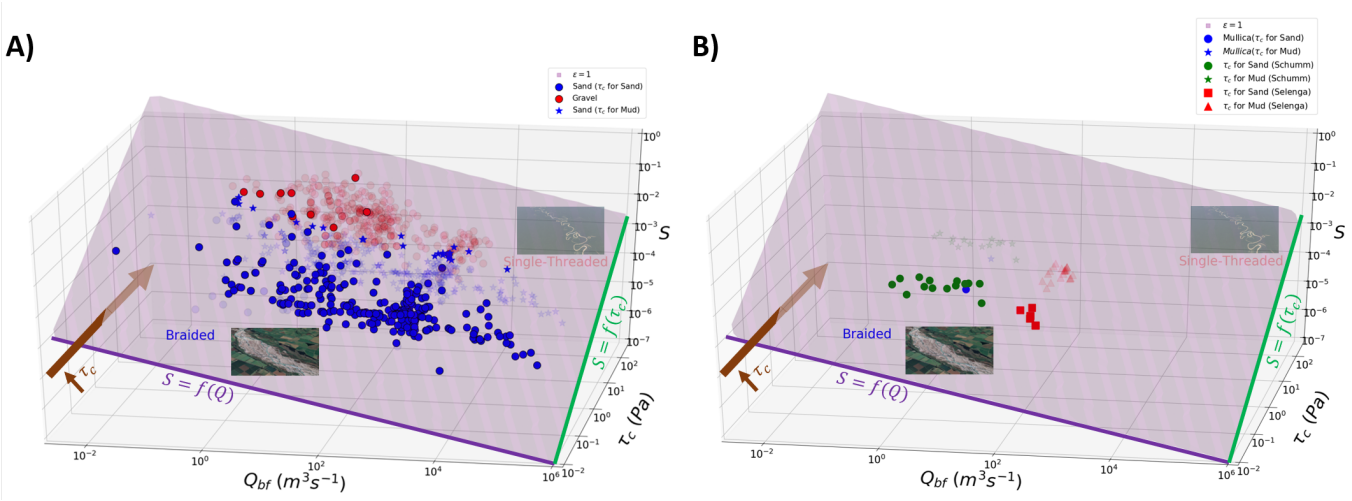

Figure 4: Planform pattern morphospace of alluvial rivers in the global dataset. A) Global data set: Hydrodynamic stability criterion $\epsilon = 1$, shown by the plane, shows the expected separation of braided from single-threaded channels in the parameter space of discharge Q_{bf}, slope S and entrainment threshold τ_c. Inset images show typical braided morphology of the Waimakariri River, and single-threaded meandering Rio Purus (Image Sources: Google Earth). Virtually all rivers in this dataset should plot as single-threaded. When τ_c for bed-sediment D_{50} determined from the Shields curve is used, gravel-bedded rivers almost invariably plot as single-thread, but fine-grained rivers are mostly braided. Using a representative $\tau_c = 8$ Pa for mud instead, fine-grained rivers shift to the correct single-threaded morphospace. Purple line highlights $Q_{bf} - S$ relation for a given τ_c, which follows the classic empirical delineation [25]. Green line indicates $\tau_c - S$ relations for a given Q_{bf}. Brown arrow shows how increasing τ_c can drive migration across the $\epsilon = 1$ plane. B) Additional single-threaded rivers with sand beds and muddy banks, in which τ_c of bank-toe was measured (Mullica) or could be estimated from reported descriptions of bank material [26] (Schumm and Selenga). Selenga River delta channels were selected so as to be outside of the range of the backwater effect [27], and additional rivers were reported by Schumm [28].

may improve channel geometry predictions; to first order, however, one may assume $C_f \sim 10^1$ Fig. S1). The Parker closure for gravel-bedded rivers can be extended to finer-grained systems, by explicitly accounting for τ_c of the threshold limiting bank material. This framework also illustrates how changing river-bank composition may induce a change in planform morphology from braiding to meandering, which has implications for interpreting alluvial river deposits on Earth and Mars [11]. The apparent success of the threshold limiting model raises some intriguing questions. This approach is purely hydraulic: channel geometry is determined by the conveyance capacity of water and the entrainment threshold of the channel margins. Sediment supply, however, has been proposed to influence channel geometry [6] and also planform morphology [29]. We posit that there is in fact an indirect influence of sediment supply, through its modulation of slope (see Supplementary Materials). On engineering (decadal) timescales, slope is often considered an independent variable because its timescale of adjustment is much slower than width and depth [30, 15]. Over longer timescales, however, slope adjusts to accommodate the sediment load imposed by the channel basin [30]. Any changes in the grain size of sediment supplied to a river will have more immediate impact on channel geometry by altering τ_c. Despite these unresolved issues, the simple model equations 1 and 2 may find immediate use in engineering applications. Management and restoration of river channels requires an understanding of the relations between hydraulics and channel geometry [12], and we suggest that first-order predictions from the threshold-limiting model represent useful design criteria.

METHODS

We utilised Google Earth's ruler tool to collect measurements of W_{bf} for the Lochsa River. Images of the channel were not necessarily taken at bankfull conditions, so bankfull extent was estimated based on color variations with an approximate pixel resolution of 0.65 m. Measurements of Q_{bf}, S, D_{50}, and τ_c for the Lochsa River were reported in the Supplementary Material of Phillips and Jerolmack, 2016 [15]. The global dataset we utilised has been presented elsewhere [8]. It contains measured channel geometry and discharge values associated with bankfull flow; i.e., when the channel is completely filled with water. Friction factor C_f for each river was computed using a Darcy-Weisbach flow resistance relation (Supplementary Material). Estimates for the threshold entrainment stress (τ_c) of non-cohesive sediment were determined from an empirical fit to the Shields curve [23], which represents the combined fluid drag and lift forces required to overcome particle friction. Channel geometry and bank composition data for rivers presented in figure 4B were taken from reported values in the associated publications [27, 4]. Estimates of threshold entrainment stress for cohesive sediment in these additional rivers were calculated using an empirical relation between τ_c and %silt-clay [26].

Data to produce the hydrograph magnitude-frequency curves (Fig. 2B,C) were collected from the USGS website and analysed using code and methodology developed by Phillips and Jerolmack, 2016 [15]. Gravel-bedded rivers were the same rivers analysed by Phillips and Jerolmack, 2016 [15]; we added fine-grained rivers from global data set [8] for which sufficient data were available. Because of heavy overlap between the gravel- and fine-grained rivers, only the mean for fine-grained rivers and standard deviation for gravel-bedded rivers are shown.

The Mullica River was selected for field work due to its proximity, and desired bed and bank properties for the study. Channel slope for the studied reach was determined over a 6-km stretch of river using a Trimble ProXH differential GPS sampling at 1 Hz from a boat (Supplementary Fig. 3). Bed grain size was relatively uniform throughout the reach, and was measured using a CAMSIZER (Supplementary Fig. 4). We surveyed bankfull channel width and depth at 18 cross sections using a laser range finder (Supplementary Fig. 5). Calculations of bankfull stress at each location utilised the bankfull depth at each cross section, and the reach-averaged slope. At each cross section, the edge of the bank was identified in the field. Bank-toe erodibility measurements were made using the Mudbuster *in-situ* erodibility tester, following the procedures and calibrations outlined in another paper [22]. At each cross section, four measurements of τ_c were taken at the toe of the channel bank. Fluid shear stress is systematically increased with the Mudbuster while turbidity is measured using two photo-diodes. Increased turbidity measures as a voltage drop, which is expected to occur abruptly at a threshold fluid stress. While each measurement showed a voltage decline with increasing applied shear stress, determining a precise threshold was challenging due to noise (Fig. S6). Variations of the voltage drop from measurements within a single cross section, and measurements among different cross sections, were of comparable magnitude (Supplementary Fig. 6). Accordingly, we lumped together all voltage drop curves to produce a more robust statistical determination of the average τ_c for all cross sections (Fig. 4C). This is the reach-averaged value $\tau_c = 4.5$ Pa reported in the text.

REFERENCES

[1] Gary Parker. Self-formed straight rivers with equilibrium banks and mobile bed. part 2. the gravel river. *Journal of Fluid mechanics*, 89(1):127–146, 1978. doi: 10.1017/S0022112078002505.

[2] Gary Parker. On the cause and characteristic scales of meandering and braiding in rivers. *Journal of fluid mechanics*, 76(3): 457–480, 1976. doi: 10.1017/S0022112076000748.

[3] Wilhelm Ripl. Water: the bloodstream of the biosphere. *Philosophical Transactions of the Royal Society of London. Series B: Biological Sciences*, 358(1440):1921–1934, 2003.

[4] SA Schumm. The shape of alluvial channels in relation to sediment type. *USGS Prof. Pap*, 1960.

[5] Brett C Eaton and Michael Church. Predicting downstream hydraulic geometry: a test of rational regime theory. *Journal of Geophysical Research: Earth Surface*, 112(F3025), 2007. doi: 10.1029/2006JF000734.

[6] Allison M Pfeiffer, Noah J Finnegan, and Jane K Willenbring. Sediment supply controls equilibrium channel geometry in gravel rivers. *Proceedings of the National Academy of Sciences*, 114(13):3346–3351, 2017.

[7] Luna Bergere Leopold and Thomas Maddock. *The hydraulic geometry of stream channels and some physiographic implications*, volume 252. US Government Printing Office, 1953.

[8] Kieran BJ Dunne and Douglas J Jerolmack. Evidence of, and a proposed explanation for, bimodal transport states in alluvial rivers. *Earth Surface Dynamics*, 6(3):583–594, 2018. doi: 10.5194/esurf-6-583-2018.

[9] William E Dietrich, J Dungan Smith, and Thomas Dunne. Flow and sediment transport in a sand bedded meander. *The Journal of Geology*, 87(3):305–315, 1979.

[10] Peter Wilcock. Friction between science and practice: The case of river restoration. *Eos, Transactions American Geophysical Union*, 78(41):454–454, 1997.

[11] Vamsi Ganti, Alexander C Whittaker, Michael P Lamb, and Woodward W Fischer. Low-gradient, single-threaded rivers prior to greening of the continents. *Proceedings of the National Academy of Sciences*, 116(24):11652–11657, 2019.

[12] Martin W Doyle, Doug Shields, Karin F Boyd, Peter B Skidmore, and DeWitt Dominick. Channel-forming discharge selection in river restoration design. *Journal of Hydraulic Engineering*, 133(7):831–837, 2007.

[13] Andrew P Nicholas. Modelling the continuum of river channel patterns. *Earth Surface Processes and Landforms*, 38(10): 1187–1196, 2013.

[14] National Research Council et al. *Landscapes on the edge: New horizons for research on Earth's surface*. national academies Press, 2010.

[15] Colin B Phillips and Douglas J Jerolmack. Self-organization of river channels as a critical filter on climate signals. *Science*, 352(6286):694–697, 2016. doi: 10.1126/science.aad3348.

[16] François Métivier, Eric Lajeunesse, and Olivier Devauchelle. Laboratory rivers: Lacey's law, threshold theory, and channel stability. *Earth Surface Dynamics*, 5(1):187–198, 2017. doi: 10.5194/esurf-5-187-2017.

[17] Leo P Kadanoff. More is the same; phase transitions and mean field theories. *Journal of Statistical Physics*, 137(5-6):777, 2009.

[18] Gregory V Wilkerson and Gary Parker. Physical basis for quasi-universal relationships describing bankfull hydraulic geometry of sand-bed rivers. *Journal of Hydraulic Engineering*, 137(7):739–753, 2010.

[19] Gary Parker. Self-formed straight rivers with equilibrium banks and mobile bed. part 1. the sand-silt river. *Journal of Fluid Mechanics*, 89(1):109–125, 1978.

[20] SM Trampush, S Huzurbazar, and Brandon McElroy. Empirical assessment of theory for bankfull characteristics of alluvial channels. *Water Resources Research*, 50(12):9211–9220, 2014.

[21] Chuan Li, Matthew J Czapiga, Esther C Eke, Enrica Viparelli, and Gary Parker. Variable shields number model for river bankfull geometry: bankfull shear velocity is viscosity-dependent but grain size-independent. *Journal of Hydraulic Research*, 53(1):36–48, 2015.

[22] Kieran B.J. Dunne, Paulo E. Arratia, and Doulgas J. Jerolmack. A new method for in-situ measurement of the erosion threshold of river channels. 2019.

[23] Leo C van Rijn. Initiation of motion and suspension; critical bed-shear stress for sand-mud mixtures. 2016. URL www.leovanrijn-sediment.com.

[24] Michal Tal and Chris Paola. Dynamic single-thread channels maintained by the interaction of flow and vegetation. *Geology*, 35(4):347–350, 2007.

[25] Luna Bergere Leopold and Markley Gordon Wolman. *River channel patterns: braided, meandering, and straight*. US Government Printing Office, 1957.

[26] Jason P Julian and Raymond Torres. Hydraulic erosion of cohesive riverbanks. *Geomorphology*, 76(1-2):193–206, 2006. doi: 10.1016/j.geomorph.2005.11.003.

[27] Tian Y Dong, Jeffrey A Nittrouer, Matthew J Czapiga, Hongbo Ma, Brandon McElroy, Elena Il'icheva, Maksim Pavlov, Sergey Chalov, and Gary Parker. Roles of bank material in setting bankfull hydraulic geometry as informed by the selenga river delta, russia. *Water Resources Research*, 2019.

[28] Stanley A Schumm. Sinuosity of alluvial rivers on the great plains. *Geological Society of America Bulletin*, 74(9):1089–1100, 1963. doi: 10.1130/0016-7606(1963)74[1089:SOAROT]2.0.CO;2.

[29] BC Eaton, Robert G Millar, and Sarah Davidson. Channel patterns: Braided, anabranching, and single-thread. *Geomorphology*, 120(3-4):353–364, 2010.

[30] Chris Paola, Gary Parker, Rebecca Seal, Sanjiv K Sinha, John B Southard, and Peter R Wilcock. Downstream fining by selective deposition in a laboratory flume. *Science*, 258(5089):1757–1760, 1992.

AUTHOR CONTRIBUTIONS STATEMENT

K.B.J.D performed the research and analysed the data, D.J.J. supervised the research, and both authors wrote the paper.

ACKNOWLEDGEMENTS

We thank James Pizzuto, Jeffrey Nittrouer, and Colin Phillips for their feedback that helped us frame aspects of this paper. We thank Colin Phillips for sharing his hydrograph analysis code. The research was sponsored by the Army Research Laboratory and the National Science Foundation, and was accomplished under grant numbers W911-NF-16-1-0290 and 1734355, respectively. All data generated during this study are included in the supplementary information files.